was also interpreted in terms of $S = {}^5/_2$ only, with weak antiferromagnetic exchange.[19] This apparently takes place mainly via ligand-delocalized electron spin density.[19] A similar process could account for the anomalously low magnetic moments in the present, solvated, complexes. The results of this work (Figure 3) represent the first unambiguous spectroscopic evidence for the idea that solvation by nonpolar, non-hydrogen-bonding species favor the spin-doublet ground state in tris(dialkyldithiocarbamato)iron(III) systems. In the present case, this occurs for one that is clearly a spin sextet at all T for its unsolvated form. However, it still appears to be the case that the sextet and doublet are not distinguished via Mössbauer spectroscopy in the rapidly relaxing paramagnetic-temperature region. Whether or not this is due to (1) an extraordinary accidental similarity of the parameters (δ, ΔE) for the ^{6}A and ^{2}T states or (2) more likely dynamic rapid interconversion between them is also not clear from the present study.

Acknowledgment. We are pleased to acknowledge the support from National Science Foundation Grants DMR-80-16441 and CHE77-01372.

Registry No. Tris(morpholinecarbodithioato)iron(III), 14285-01-9; tris(pyrrolidinecarbodithioato)iron(III), 21288-86-8.

(19) Cukauskas, E. J.; Deaver, B. S., Jr.; Sinn, E. *J. Chem. Soc., Chem. Commun.* **1974**, 698.

Contribution from the Departments of Chemistry, Howard University, Washington, D.C. 20059, University of New Orleans, New Orleans, Louisiana, and University of Virginia, Charlottesville, Virginia 22901

Antiferromagnetically and Ferromagnetically Coupled Nickel(II) Dimers with and without Interdimer Coupling. Solvent Effects in the Preparation of Nickel(II) Dimers[1]

RAY J. BUTCHER,[2a] CHARLES J. O'CONNOR,[2b] and EKK SINN*[2c]

Received May 23, 1980

The structural and magnetic properties are reported for a group of chemically similar nickel(II) dimers with salicylaldimine ligands. Three general categories of compounds may be prepared for a variety of bidentate Schiff base (sb) nickel(II) complexes that have the same general formula $[Ni(sb)(NO_3)L]_2$ and differ only in structural details and the type of Lewis acid solvent molecule (L) that is present during crystallization. Antiferromagnetic interactions are observed when the central Ni_2O_2 bridging group is approximately coplanar with the principal sb ligand plane. Ferromagnetic interactions are observed when these planes are approximately orthogonal. When L = C_2H_5OH, hydrogen bonding between L and the NO_3 groups of neighboring molecules forms an antiferromagnetic pathway along infinite chains of ferromagnetic dimers. The three categories are represented by the following complexes. $[Ni(ps)(NO_3)(2\text{-pic})]_2\cdot CH_2Cl_2$ (ps = phenylsalicylaldimine): crystal data space group $P\bar{1}$, $Z = 1$, $a = 9.424$ (2) Å, $b = 11.327$ (3) Å, $c = 11.468$ (3) Å, $\alpha = 117.96$ (2)°, $\beta = 90.29$ (3)°, $\gamma = 91.62$ (2)°, $V = 1081$ Å^3, $R = 4.5\%$ for 2342 reflections; magnetic data $g = 2.12$, $J = 8.7$ cm^{-1}, $D \approx 13$ cm^{-1} ($zJ' = 0.07$). $[Ni_2(ips)_2(NO_3)_2(EtOH)_2]_\infty$ (ips = isopropylsalicylaldimine): crystal data space group $P\bar{1}$, $Z = 1$, $a = 9.161$ (5) Å, $b = 9.183$ (2) Å, $c = 13.353$ (7) Å, $\alpha = 128.25$ (3)°, $\beta = 93.72$ (4)°, $\gamma = 110.44$ (3)°, $V = 764$ Å^3, $R = 3.1\%$ for 1851 reflections; magnetic data $g = 2.15$, $J = 16.0$ cm^{-1}, $D \approx 15$ cm^{-1} ($zJ' = 0.14$). $[Ni(ips)(NO_3)DMF]_2$: crystal data space group $P\bar{1}$, $Z = 1$, $a = 9.506$ (2) Å, $b = 10.095$ (4) Å, $c = 10.588$ (3) Å, $\alpha = 94.80$ (2)°, $\beta = 126.59$ (2)°, $\gamma = 92.70$ (2)°, $V = 807$ Å^3, $R = 5.5\%$ for 2039 reflections; magnetic data $g = 2.32$, $J = -9.2$ cm^{-1}, $D \approx 12$ cm^{-1}. The magnetic behavior is correlated with differences in exchange pathways as obtained from the crystal structures. Although it is demonstrated that D and zJ' cannot be estimated accurately from the magnetic data, the values of the intradimer interaction, J, are reliable.

Introduction

Copper complexes of bidentate Schiff bases are well-known to form binuclear antiferromagnetic copper(II) complexes of the types **1**.[3] The geometry of the copper complexes positions

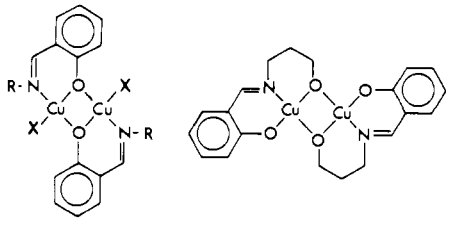

1

the salicylaldimine residue approximately parallel to the Cu_2O_2 bridge. Nickel(II) dimers containing salicylaldimine ligands have been prepared; however, the only analogous nickel(II) complexes known to date have the salicylaldimine residues at right angles to the Ni_2O_2 bridge and a ferromagnetic intradimer exchange interaction.

Nickel complexes of bidentate Schiff bases $Ni(bsb)_2$ such as with salicylaldimines (sal) or chlorobenzophenones (cbp) react with nickel nitrate in triethyl orthoformate (TEOF) or ethanol to form binuclear complexes $[Ni_2(bsb)_2(NO_3)_2(EtOH)_2]$ of the type **2**.[4-6] Hydrogen bonding between the

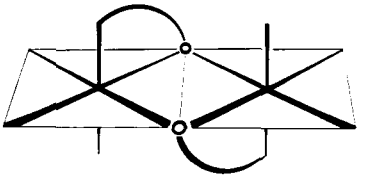

2, "cis"

ethanolic OH and the nitrato ligands of adjacent nickel binuclears leads to infinite chains of the neutral dinickel units.

(1) Paper presented at the 176th National Meeting of the American Chemical Society, Miami, Fla., Sept 1978; see Abstracts, No. INOR 102.

(2) (a) Howard University. (b) University of New Orleans. (c) University of Virginia.

(3) Robinson, W. T.; Sinn, E. *J. Chem. Soc., Chem. Commun.* **1972**, 359. Gluvchinsky, P.; Mockler, G. M.; Healy, P. C.; Sinn, E. *J. Chem. Soc., Dalton Trans.* **1974**, 1156. Countryman, R. M.; Robinson, W. T.; Sinn, E. *Inorg. Chem.* **1974**, *13*, 2013. Sinn, E. *J. Chem. Soc., Chem. Commun.* **1975**, 665. Sinn, E. *Inorg. Chem.* **1976**, *15*, 358. Davis, J. A.; Sinn, E. *J. Chem. Soc., Dalton Trans.* **1976**, 165. Butcher, R. J.; Sinn, E. *Inorg. Chem.* **1976**, *15*, 1604.

(4) Butcher, R. J.; Sinn, E. *J. Chem. Soc., Chem. Commun.* **1975**, 832.

(5) Butcher, R. J.; Jasinski, J.; Mockler, G. M.; Sinn, E. *J. Chem. Soc., Dalton Trans.* **1976**, 1099.

(6) Butcher, R. J.; Sinn, E. *Aust. J. Chem.* **1979**, *32*, 331.

0020-1669/81/1320-3486$01.25/0

Modification of the Schiff base ligand so as to reduce the steric constraints can produce trinuclear molecules.[1,7] It is of interest to substitute other Lewis base ligands for ethanol, to remove the possibility of polymeric hydrogen-bonded linking, and to compare the magnetic properties in the presence and absence of hydrogen bonding. Also it would be of interest to synthesize nickel analogues more similar to the copper complexes. This would be a nickel complex of type **3**, which has the oxygen

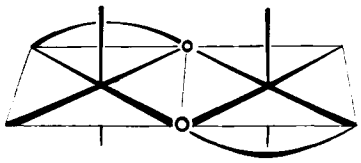

3, "trans"

bonding approximately planar (sp^2) and the salicylaldimine ligands approximately parallel to the Ni_2O_2 bridge. The analogy is restricted only by the fact that the nickel atoms must be five- or six-coordinated in order to be paramagnetic rather than four-coordinated as in the case of the copper complexes.

We have undertaken the synthesis and characterization of a series of nickel(II) dimers of the general formula $[Ni(R\text{-}sal)NO_3R']_2$, initially with the aim of studying the effects of interdimer hydrogen bonding on the magnetic susceptibility of the ferromagnetic dimers. However, the investigation unexpectedly resulted in the successful synthesis of an antiferromagnetically coupled nickel(II) dimer, type **3**.

The gross magnetic and structural features of the entire series of dimers may be divided into three general categories: (a) insulated ferromagnetic dimers, type **2** structure; (b) hydrogen-bonded ferromagnetic dimers, type **2** structure; (c) antiferromagnetic dimers, type **3** structure.

We report here on the syntheses, crystal structures, and magnetic properties of three compounds: $[Ni(ps)(NO_3)(2\text{-}pic)]_2$, case a; $[Ni_2(ips)_2(NO_3)_2(EtOH)_2]_\infty$, case b; and $[Ni(ips)(NO_3)DMF]_2$, case c, where ps = *N*-phenylsalicylaldimine, ips = *N*-isopropylsalicylaldimine, and 2-pic = 2-methylpyridine.

Experimental Section

Synthesis of Compounds. (a) $[Ni(ps)(NO_3)(2\text{-}pic)]_2\cdot 2CH_2Cl_2$. $Ni(ps)_2$ (0.001 mol) was dissolved in 100 mL of dichloromethane plus 5–10 mL of TEOF. $Ni(NO_3)_2\cdot 6H_2O$ (0.0015 mol) was dissolved in 50 mL of TEOF, and the two solutions were mixed, resulting in a clear, light green solution. 2-Picoline (0.003 mol) was then added dropwise from a syringe to the rapidly stirred solution. The resulting solution was then heated and stirred for 15 min, filtered, and allowed to slowly evaporate. Single crystals suitable for X-ray analysis resulted after 5–6 days.

(b) $[Ni_2(ips)_2(NO_3)_2(EtOH)_2]$. $Ni(ips)_2$ (0.01 mol) was dissolved in chloroform. $Ni(NO_3)_2\cdot 6H_2O$ (0.01 mol) was dissolved in a 1:1 solution of ethanol–TEOF. The solutions were mixed and allowed to evaporate slowly. Single crystals suitable for X-ray analysis were obtained.

(c) $[Ni(ips)(NO_3)DMF]_2$. One centimolar quantities of $Ni(ips)_2$ and $Ni(NO_3)_2\cdot 6H_2O$ were each dissolved in DMF. The solutions were mixed, and single crystals were obtained by allowing the resulting solution to slowly evaporate in a sulfuric acid desiccator.

The infrared spectra of the complexes provide additional characterization for the complexes[5] and will be described elsewhere.

Magnetic Measurements. The magnetic susceptibilities were measured as fields of about 100 G and at temperatures ranging from 4 to 100 K with use of a superconducting susceptometer. In each case, the polycrystalline samples were used for magnetic susceptibility measurements. Calibration and measuring techniques are described elsewhere.[8,9]

Crystal Data for $[Ni(ps)(NO_3)(2\text{-}pic)]_2\cdot 2CH_2Cl_2$ (a): $Ni_2Cl_4O_8N_6C_{40}H_{38}$, mol wt 990, space group $P\bar{1}$, $Z = 1$, $a = 9.424$ (2) Å, $b = 11.327$ (3) Å, $c = 11.468$ (3) Å, $\alpha = 117.96$ (2)°, $\beta = 90.29$ (3)°, $\gamma = 91.62$ (2)°, $V = 1081$ Å^3, $\rho_{calcd} = 1.57$ g cm^{-3}, $\rho_{obsd} = 1.54$ g cm^{-3}, μ(Mo Kα) = 11.8 cm^{-1}; crystal dimensions (distances in mm of faces from centroid) (110) 0.08, ($\bar{1}\bar{1}0$) 0.08, ($1\bar{1}0$) 0.08, ($\bar{1}10$) 0.08, (001) 0.10, (00$\bar{1}$) 0.10; maximum, minimum transmission coefficients 0.91, 0.89.

Crystal Data for $[Ni_2(ips)_2(NO_3)_2(EtOH)_2]_\infty$ (b): $Ni_2O_{10}N_4C_{20}H_{18}$, mol wt 658, space group $P\bar{1}$, $Z = 1$, $a = 9.161$ (5) Å, $b = 9.183$ (2) Å, $c = 13.353$ (7) Å, $\alpha = 128.25$ (3)°, $\beta = 93.72$ (4)°, $\gamma = 110.44$ (3)°, $V = 764$ Å^3, $\rho_{calcd} = 1.43$ g cm^{-3}, $\rho_{obsd} = 1.39$ g cm^{-3}, μ(Mo Kα) = 12.8 cm^{-1}; crystal dimensions (mm from centroid) (100) 0.17, (100) 0.17, (011) 0.40, (011) 0.40, (001) 0.045, (001) 0.045; maximum, minimum transmission coefficients 0.92, 0.75.

Crystal Data for $[Ni(ips)(NO_3)DMF]_2$ (c): $Ni_2O_{10}N_6C_{26}H_{38}$, mol wt 680, space group $P\bar{1}$, $Z = 1$, $a = 9.506$ (2) Å, $b = 10.095$ (4) Å, $c = 10.588$ (3) Å, $\alpha = 94.80$ (2)°, $\beta = 126.59$ (2)°, $\gamma = 92.70$ (2)°, $V = 807$ Å^3, $\rho_{calcd} = 1.40$ g cm^{-3}, $\rho_{obsd} = 1.38$ g cm^{-3}, μ(Mo Kα) = 12.2 cm^{-1}; crystal dimensions (mm from centroid) (100) 0.15, ($\bar{1}00$) 0.15, (010) 0.105, ($0\bar{1}0$) 0.105, (001) 0.11, (00$\bar{1}$) 0.11; maximum, minimum transmission coefficients 0.87, 0.82.

Collection of Data. Cell dimensions and space group data were obtained by standard methods on an Enraf-Nonius four-circle CAD-4 diffractometer. The θ–2θ scan technique was used, as previously described,[10] to record the intensities for all nonequivalent reflections for which $1° < 2\theta < 47°$ for $[Ni(ps)(NO_3)(2\text{-}pic)]_2$, $1° < 2\theta < 46°$ for $[Ni_2(ips)_2(NO_3)_2(EtOH)_2]_\infty$, and $1° < 2\theta < 46°$ for $[Ni(ips)(NO_3)DMF]_2$. Scan widths were calculated as $(A + B \tan\theta)$, where A is estimated from the mosaicity of the crystal and B allows for the increase in width of peak due to $K\alpha_1$–$K\alpha_2$ splitting. The values for A and B were 0.6 and 0.35°, respectively, for all three complexes.

The intensities of four standard reflections, monitored for each crystal at 100-reflection intervals, showed no greater fluctuations than those expected from Poisson statistics. The raw intensity data were corrected for Lorentz–polarization effects and absorption. Of the 2784 independent intensities for $[Ni(ps)(NO_3)(2\text{-}pic)]_2$, 2014 for $[Ni_2(ips)_2(NO_3)_2(EtOH)_2]_\infty$, and 2123 for $[Ni(ips)(NO_3)DMF]_2$, there were 2342, 1851, and 2039, respectively, with $F_o^2 > 3\sigma(F_o^2)$, where $\sigma(F_o^2)$ was estimated from counting statistics.[11] These data were used in the final refinement of the structural parameters.

Structure Determinations. The positions of the nickel atoms and some ligand oxygen atoms were located from three-dimensional Patterson functions. The intensity data were phased sufficiently well by these positional coordinates to permit location of the other nonhydrogen atoms from Fourier syntheses. Full-matrix least-squares refinement was carried out as previously described.[10] Anisotropic temperature factors were introduced for all nonhydrogen atoms. Further Fourier difference functions permitted location of the hydrogen atoms, which were included in the refinement for three cycles of least squares and then held fixed. The models coverged with $R = 4.5\%$ and $R_w = 4.8\%$ for $[Ni(ps)(NO_3)(2\text{-}pic)]_2$, $R = 3.1\%$ and $R_w = 3.8\%$ for $[Ni_2(ips)_2(NO_3)_2(EtOH)_2]_\infty$, and $R = 5.5\%$ and $R_w = 7.1\%$ for $[Ni(ips)(NO_3)DMF]_2$. Final Fourier difference functions were featureless. Tables of the observed and calculated structure factors are available.[12] The principal programs used are as previously described.[10]

Results and Discussion

Final positional and thermal parameters for the three complexes are given in Table I. Tables II and III contain the bond lengths and angles. The digits in parentheses in the tables are the estimated standard deviations in the least significant figures quoted and were derived from the inverse matrix in the course of least-squares refinement calculations. Figure 1 shows a stereopair view of the $[Ni(ps)(NO_3)(2\text{-}pic)]_2$ molecule, while Figure 2 shows the molecular packing in the unit cell. Figure

(7) Butcher, R. J.; Sinn, E., to be submitted for publication.
(8) O'Connor, C. J.; Sinn, E.; Cukauskas, E. J.; Deaver, B. S., Jr. *Inorg. Chim. Acta* **1979**, *32*, 29.
(9) O'Connor, C. J.; Sinn, E.; Deaver, B. S., Jr.; Fariss, T. L.; Bucelot, T.; Galfor, C., to be submitted for publication.
(10) Freyberg, D. P.; Mockler, G. M.; Sinn, E. *J. Chem. Soc., Dalton Trans.* **1976**, 447.
(11) Corfield, P. W. R.; Doedens, R. J.; Ibers, J. A. *Inorg. Chem.* **1967**, *6*, 197.
(12) Supplementary material.

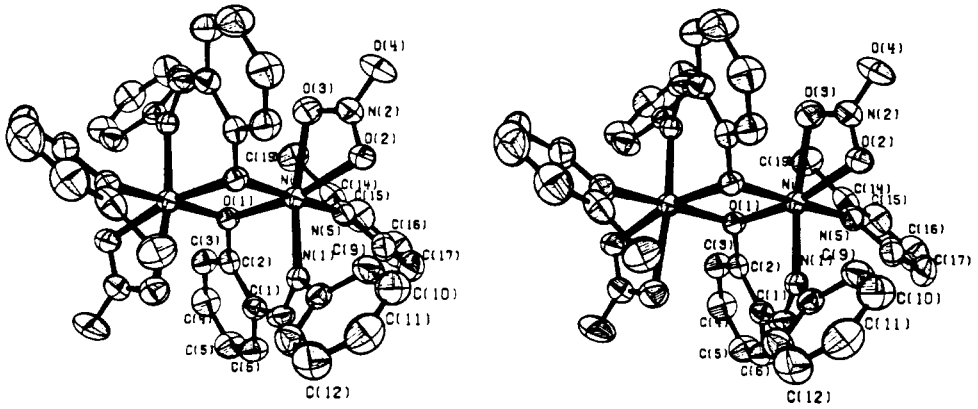

Figure 1. Stereoview of the $[Ni(ps)(NO_3)(2\text{-pic})]_2$ molecule, "cis" structure **2**, insulated ferromagnetic dimer (type a).

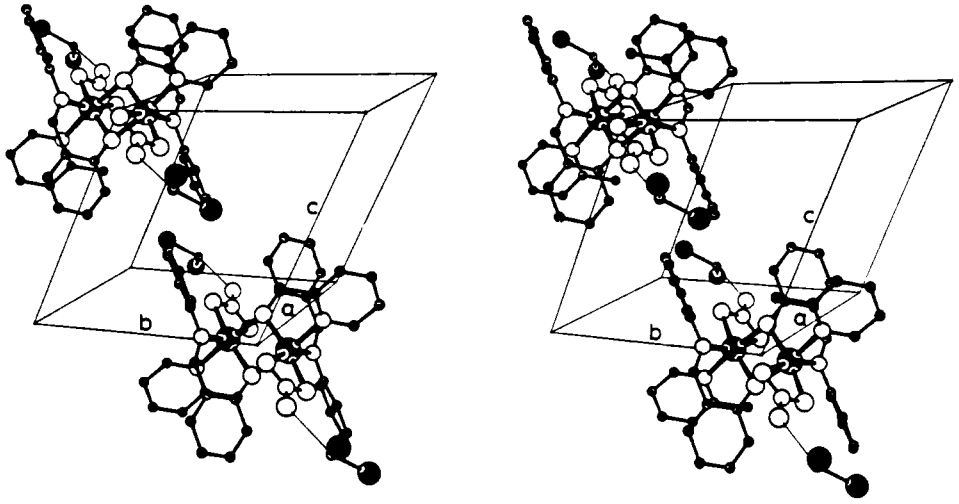

Figure 2. Molecular packing in the unit cell for $[Ni(ps)(NO_3)(2\text{-pic})]_2 \cdot 2CH_2Cl_2$.

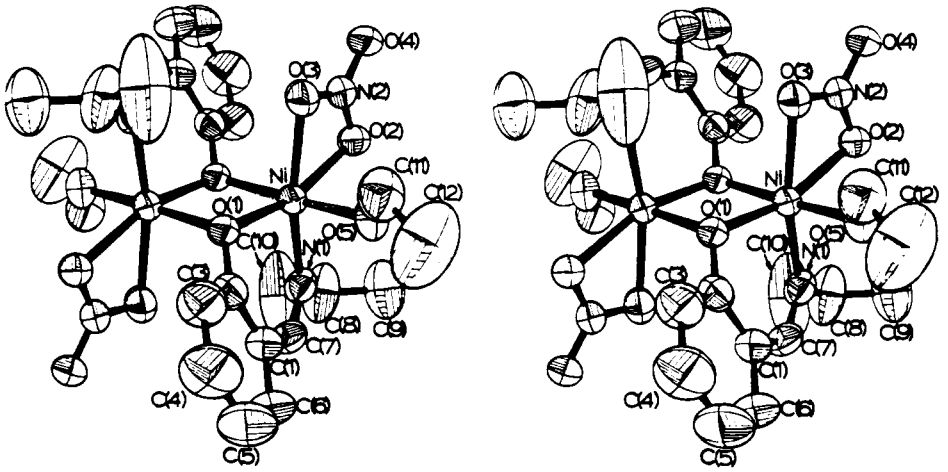

Figure 3. Stereoview of the $[Ni(ips)(NO_3)(EtOH)]_2$ molecule, "cis" structure **2**, hydrogen-bonded ferromagnetic dimer (type b).

3 is a stereoview of the $[Ni_2(ips)_2(NO_3)_2(EtOH)_2]$ unit, while Figure 4 shows the packing of the infinite $[Ni_2(ips)_2(NO_3)_2(EtOH)_2]_\infty$ in the crystal lattice. Figures 5 and 6 show stereoviews of the $[Ni(ips)(NO_3)DMF]_2$ molecule and molecular packing, respectively.

The complexes $[Ni(ps)(NO_3)(2\text{-pic})]_2$, case a, and $[Ni_2(ips)_2(NO_3)_2(EtOH)_2]_\infty$, case b, are quite similar in structure except that the former consists of discrete binuclear complex molecules and the latter has hydrogen-bonding links between the ethanolic hydroxyl and the nitrato ligands of adjacent binuclear units to form infinite chains. $[Ni(ips)(NO_3)DMF]_2$, case c, consists of discrete binuclear molecules but differs from the other two complexes in the region of the nickel atoms. The main difference is that in case c the Ni_2O_2 bridging plane is essentially coplanar with the planes of salicylaldimine ligands as in **2** (cis), while in cases a and b these two planes are essentially orthogonal, as in **3** (trans). This is achieved by a rotation of the Schiff base ligand about the phenolic O(1)–C(2) bond so as to allow bonding of the imine nitrogen atom within the Ni_2O_2 plane in $[Ni(ips)(NO_3)DMF]_2$ and perpendicular to Ni_2O_2 in $[Ni(ps)(NO_3)(2\text{-pic})]_2$ and $[Ni_2(ips)_2(NO_3)_2(EtOH)_2]_\infty$. This produces an increase of just over 4° in the Ni–O(1)–C(2) angles. The two angles are quite similar in the cis complexes: 118.9 (3) and 124.6 (3)° in a, 119.4 (1) and 124.3 (1)° in b; they are larger in the trans complex c at 123.7 (1) and 128.5 (1)°.

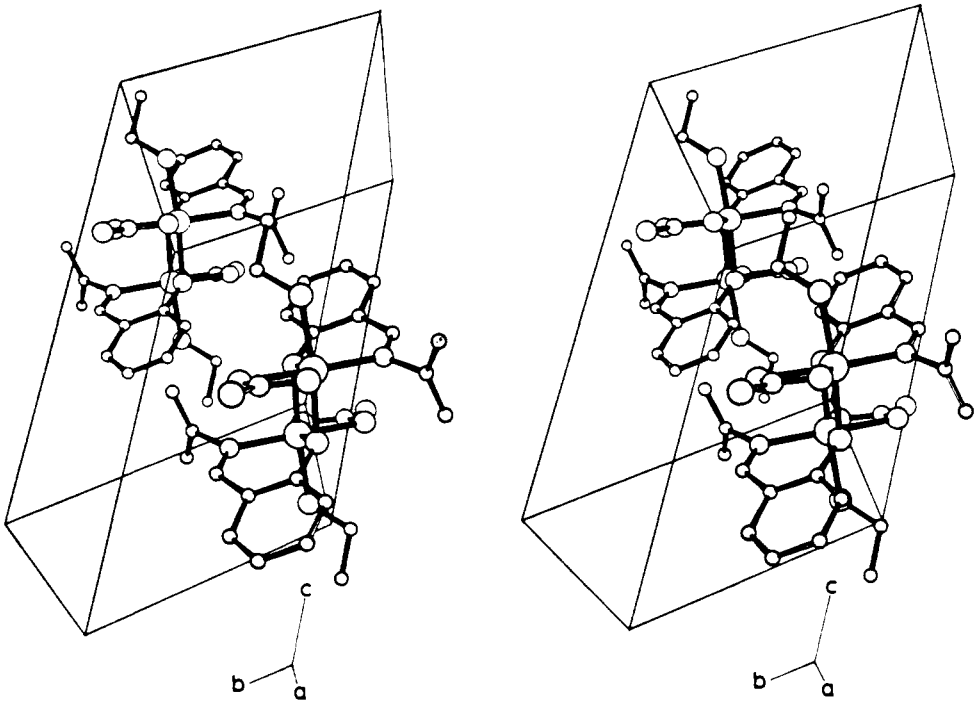

Figure 4. Molecular packing in the unit cell for $[Ni(ips)(NO_3)(EtOH)]_2$.

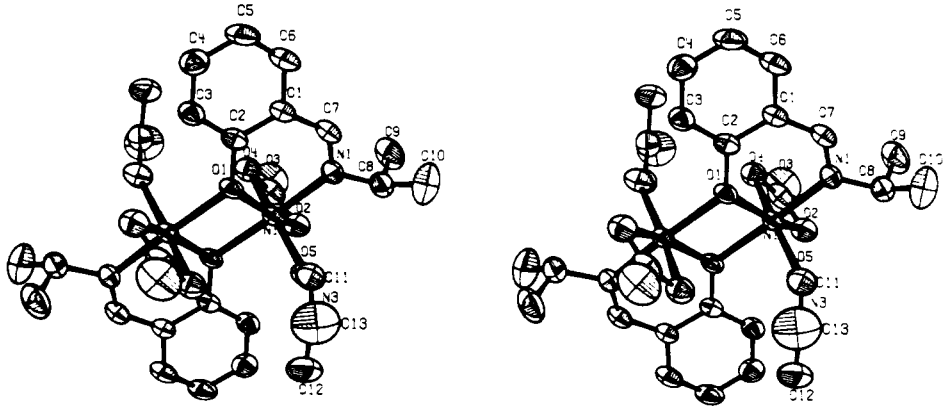

Figure 5. Stereoview of the $[Ni(ips)(NO_3)DMF]_2$ molecule, "trans" structure **3**, antiferromagnetic dimer (type c).

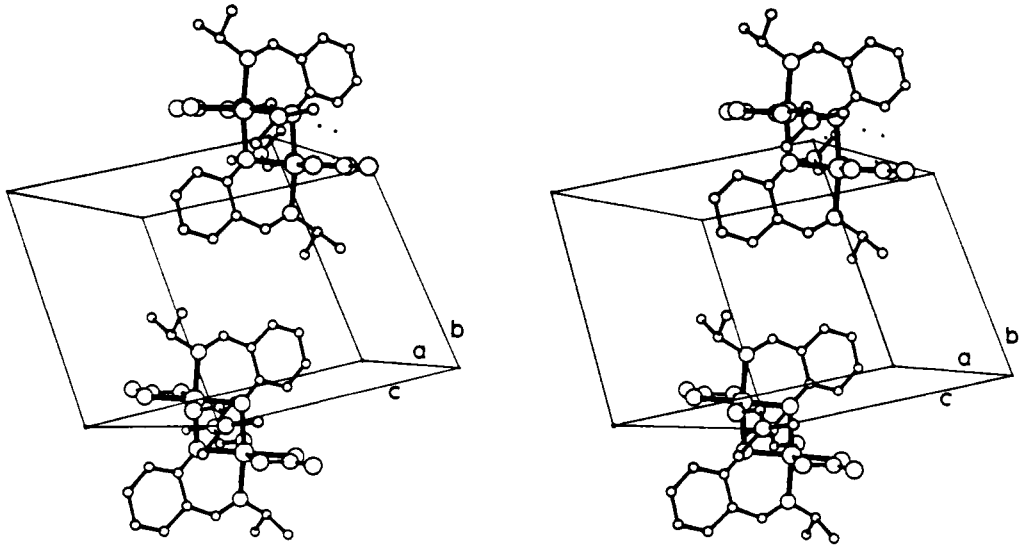

Figure 6. Molecular packing in the unit cell for $[Ni(ips)(NO_3)DMF]_2$.

Magnetic exchange in nickel(II) dimers is complicated by the fact that the crystal field splitting of the $S = 1$ ground state (D) is often the same magnitude as the electron spin-exchange parameter (J). The spin Hamiltonian that includes the terms expected to contribute to dimeric nickel(II) is shown in eq 1, where the parameters have their usual meanings.

$$H = -2JS_1 \cdot S_2 - D(S_{1z}^2 + S_{2z}^2) - g\mu_B H \cdot (S_1 + S_2) \quad (1)$$

Table I. Positional and Thermal Parameters and Their Estimated Standard Deviations[a]

a. $[Ni(ps)(NO_3)(2\text{-pic})]_2 \cdot 2CH_2Cl_2$

atom	x	y	z	B_{11}	B_{22}	B_{33}	B_{12}	B_{13}	B_{23}
Ni	−0.02711 (7)	0.13534 (5)	0.00385 (6)	2.23 (2)	2.12 (2)	2.64 (2)	0.06 (2)	−0.04 (2)	0.96 (1)
Cl(1)	0.5393 (3)	0.7041 (3)	0.3064 (2)	10.8 (2)	12.9 (1)	8.7 (1)	−3.4 (1)	−1.3 (1)	5.18 (9)
Cl(2)	0.3118 (3)	0.5888 (3)	0.1225 (3)	8.4 (2)	14.1 (2)	13.8 (1)	−2.1 (1)	−3.9 (1)	8.28 (10)
O(1)	0.0470 (3)	−0.0433 (3)	−0.1213 (3)	2.5 (1)	2.2 (1)	2.4 (1)	0.0 (1)	0.3 (1)	0.80 (8)
O(2)	−0.1508 (4)	0.2974 (3)	0.1255 (3)	2.6 (1)	2.9 (1)	4.4 (1)	0.2 (1)	0.1 (1)	1.25 (10)
O(3)	−0.2610 (4)	0.1207 (3)	−0.0202 (3)	3.6 (2)	3.7 (1)	4.0 (1)	−0.2 (1)	−0.3 (1)	1.55 (10)
O(4)	−0.3809 (4)	0.2933 (4)	0.1110 (5)	2.9 (2)	6.5 (2)	9.6 (2)	1.8 (2)	1.2 (2)	3.26 (16)
N(1)	0.1782 (4)	0.1943 (3)	0.0750 (3)	2.4 (2)	2.0 (1)	2.7 (1)	0.1 (1)	0.1 (1)	0.77 (9)
N(2)	−0.2682 (5)	0.2384 (4)	0.0731 (4)	2.8 (2)	3.9 (1)	5.2 (2)	0.7 (1)	0.4 (2)	2.62 (11)
N(5)	−0.0137 (4)	0.2063 (4)	−0.1368 (4)	3.1 (2)	3.0 (1)	3.4 (1)	0.5 (1)	0.2 (1)	1.61 (10)
C(1)	0.2760 (5)	0.0449 (4)	−0.1394 (4)	2.6 (2)	2.9 (2)	2.8 (2)	0.3 (2)	0.2 (2)	1.2 (1)
C(2)	0.1618 (5)	−0.0480 (4)	−0.1913 (4)	2.9 (2)	2.4 (1)	2.6 (2)	0.4 (2)	0.0 (2)	1.3 (1)
C(3)	0.1719 (6)	−0.1509 (5)	−0.3208 (5)	3.7 (2)	2.9 (2)	2.8 (2)	−0.1 (2)	0.1 (2)	0.6 (1)
C(4)	0.2876 (6)	−0.1573 (5)	−0.3958 (5)	4.9 (3)	4.1 (2)	2.7 (2)	0.6 (2)	0.9 (2)	0.7 (2)
C(5)	0.3983 (6)	−0.0651 (6)	−0.3452 (5)	4.0 (3)	5.0 (2)	3.8 (2)	0.3 (2)	1.4 (2)	1.7 (2)
C(6)	0.3940 (6)	0.0340 (5)	−0.2169 (5)	3.0 (2)	4.0 (2)	3.7 (2)	−0.2 (2)	0.3 (2)	1.4 (2)
C(7)	0.2834 (5)	0.1491 (5)	−0.0028 (5)	2.1 (2)	3.2 (2)	3.6 (2)	−0.6 (2)	−0.4 (2)	1.3 (1)
C(8)	0.2131 (5)	0.2832 (4)	0.2115 (4)	2.6 (2)	2.3 (2)	2.6 (2)	−0.3 (2)	−0.1 (2)	0.9 (1)
C(9)	0.1311 (6)	0.3925 (5)	0.2824 (5)	2.9 (2)	3.5 (2)	4.0 (2)	0.2 (2)	−0.4 (2)	0.9 (2)
C(10)	0.1640 (6)	0.4788 (5)	0.4129 (5)	4.1 (3)	3.6 (2)	3.7 (2)	0.0 (2)	0.4 (2)	0.2 (2)
C(11)	0.2765 (7)	0.4557 (6)	0.4745 (5)	6.0 (3)	4.4 (2)	3.1 (2)	−0.9 (2)	−0.5 (2)	0.6 (2)
C(12)	0.3580 (7)	0.3470 (6)	0.4050 (5)	5.2 (3)	5.2 (2)	4.0 (2)	0.0 (2)	−1.7 (2)	1.9 (2)
C(13)	0.3253 (6)	0.2605 (5)	0.2745 (5)	3.9 (3)	3.4 (2)	3.6 (2)	0.6 (2)	−0.2 (2)	1.1 (1)
C(14)	−0.0614 (6)	0.1395 (5)	−0.2635 (5)	3.9 (2)	4.6 (2)	3.5 (2)	1.5 (2)	0.4 (2)	2.2 (1)
C(15)	−0.0238 (7)	0.1840 (6)	−0.3521 (5)	6.2 (3)	6.2 (2)	4.3 (2)	0.8 (3)	0.0 (2)	3.0 (2)
C(16)	0.0569 (8)	0.2981 (6)	−0.3138 (6)	7.4 (4)	7.8 (2)	6.2 (2)	1.8 (3)	1.6 (3)	5.3 (2)
C(17)	0.1000 (7)	0.3702 (5)	−0.1847 (6)	5.1 (3)	4.7 (2)	7.2 (2)	0.5 (2)	1.0 (2)	4.1 (1)
C(18)	0.0615 (6)	0.3197 (5)	−0.0996 (5)	4.1 (3)	3.2 (2)	4.2 (2)	0.4 (2)	0.1 (2)	1.9 (1)
C(19)	−0.1590 (7)	0.0181 (6)	−0.3054 (5)	4.8 (3)	4.6 (2)	4.0 (2)	−0.9 (2)	−1.1 (2)	1.3 (2)
C	0.4371 (10)	0.5593 (7)	0.2071 (9)	9.0 (5)	6.9 (3)	17.0 (5)	2.5 (3)	5.4 (4)	7.3 (3)

atom	x	y	z	B, Å^2	atom	x	y	z	B, Å^2
H(3)	0.098 (5)	−0.210 (4)	−0.354 (4)	3.2 (11)	H(12)	0.429 (6)	0.331 (5)	0.444 (5)	5.1 (14)
H(4)	0.290 (6)	−0.223 (5)	−0.480 (5)	4.6 (13)	H(13)	0.374 (5)	0.195 (4)	0.237 (4)	2.4 (10)
H(5)	0.469 (6)	−0.067 (5)	−0.397 (5)	4.1 (13)	H(15)	−0.059 (6)	0.133 (5)	−0.433 (5)	5.2 (15)
H(6)	0.467 (5)	0.093 (4)	−0.175 (4)	3.1 (11)	H(16)	0.093 (7)	0.327 (6)	−0.369 (6)	7.5 (19)
H(7)	0.376 (5)	0.195 (4)	0.031 (4)	3.0 (11)	H(17)	0.159 (6)	0.450 (5)	−0.145 (5)	5.3 (15)
H(9)	0.058 (5)	0.404 (4)	0.244 (4)	2.8 (11)	H(18)	0.093 (4)	0.366 (3)	−0.015 (3)	2.2 (8)
H(19)	0.107 (6)	0.554 (5)	0.459 (5)	4.6 (14)	H(C1)	0.496 (8)	0.529 (6)	0.164 (6)	11.0 (22)
H(11)	0.299 (7)	0.510 (6)	0.559 (6)	6.6 (17)	H(C2)	0.398 (7)	0.527 (6)	0.261 (6)	7.0 (17)

b. $[Ni(ips)(NO_3)(EtOH)]_2$

atom	x	y	z	B_{11}	B_{22}	B_{33}	B_{12}	B_{13}	B_{23}
Ni	0.17204 (3)	0.04519 (4)	−0.00615 (3)	2.720 (9)	3.784 (6)	4.469 (7)	1.592 (6)	1.241 (7)	3.069 (4)
O(1)	−0.0586 (2)	−0.0899 (2)	−0.1309 (1)	3.07 (5)	3.93 (3)	4.27 (4)	1.68 (3)	1.25 (4)	3.19 (2)
O(2)	0.3860 (2)	0.0846 (2)	0.1014 (1)	3.38 (6)	4.83 (4)	6.57 (5)	1.85 (4)	1.55 (5)	4.46 (3)
O(3)	0.1658 (2)	−0.2269 (2)	−0.0478 (2)	3.67 (6)	4.74 (4)	6.65 (6)	2.11 (4)	1.90 (5)	3.99 (3)
O(4)	0.3843 (2)	−0.1842 (2)	0.0629 (2)	4.71 (6)	7.72 (4)	11.57 (6)	3.88 (4)	3.74 (5)	8.29 (3)
O(5)	0.2674 (2)	−0.0338 (2)	−0.1594 (2)	3.63 (6)	5.57 (5)	5.18 (5)	2.25 (4)	1.85 (5)	3.49 (3)
N(1)	0.2339 (3)	0.3287 (3)	0.0548 (2)	3.84 (8)	3.80 (5)	4.76 (6)	1.49 (5)	1.74 (6)	2.95 (3)
N(2)	0.3136 (2)	−0.1108 (3)	0.0390 (2)	3.50 (7)	5.57 (5)	7.04 (6)	2.64 (4)	2.55 (5)	5.05 (3)
C(1)	0.0251 (3)	0.1585 (3)	−0.1590 (2)	4.84 (9)	6.03 (6)	6.39 (7)	3.25 (6)	2.75 (7)	5.10 (4)
C(2)	−0.0803 (3)	−0.0437 (3)	−0.2064 (2)	3.89 (8)	5.20 (6)	4.69 (6)	2.61 (5)	1.78 (6)	3.70 (4)
C(3)	−0.2102 (4)	−0.1986 (4)	−0.3347 (3)	5.64 (13)	7.09 (8)	5.72 (8)	2.44 (8)	0.91 (9)	4.70 (5)
C(4)	−0.2327 (5)	−0.1597 (5)	−0.4174 (3)	8.59 (19)	11.00 (11)	6.64 (9)	3.95 (11)	0.86 (11)	6.65 (6)
C(5)	−0.1300 (5)	0.0334 (5)	−0.3742 (3)	10.25 (19)	13.36 (9)	9.50 (9)	6.60 (10)	3.89 (11)	9.96 (5)
C(6)	−0.0068 (4)	0.1902 (4)	−0.2471 (3)	7.71 (14)	8.84 (7)	9.36 (8)	4.60 (8)	4.00 (9)	8.04 (4)
C(7)	0.1602 (3)	0.3372 (3)	−0.0247 (2)	5.45 (10)	4.36 (6)	7.49 (8)	2.67 (6)	3.44 (8)	4.61 (4)
C(8)	0.3669 (4)	0.5333 (5)	0.1882 (3)	5.33 (14)	4.55 (13)	5.50 (13)	0.24 (12)	1.84 (11)	0.96 (10)
C(9)	0.5332 (5)	0.5841 (6)	0.1900 (4)	4.81 (14)	8.12 (16)	6.55 (15)	1.80 (12)	0.77 (13)	3.06 (11)
C(10)	0.3194 (6)	0.6316 (10)	0.2914 (5)	7.52 (22)	15.87 (39)	6.35 (21)	3.55 (23)	2.47 (18)	1.70 (24)
C(11)	0.1997 (4)	−0.2409 (5)	−0.2936 (3)	6.96 (14)	5.58 (10)	6.10 (11)	3.06 (9)	3.10 (10)	3.18 (7)
C(12)	0.2287 (7)	−0.2329 (8)	−0.3962 (4)	14.54 (34)	9.39 (25)	6.29 (16)	2.70 (24)	4.97 (18)	2.96 (14)

atom	x	y	z	B, Å^2	atom	x	y	z	B, Å^2
H(3)	−0.279 (3)	−0.323 (3)	−0.365 (2)	5.7 (8)	H(91)	0.542 (5)	0.537 (5)	0.110 (3)	9.9 (11)
H(4)	−0.304 (4)	−0.256 (4)	−0.494 (3)	7.9 (10)	H(92)	0.625 (4)	0.717 (4)	0.280 (3)	7.3 (9)
H(5)	−0.147 (5)	0.049 (5)	−0.434 (3)	9.7 (11)	H(93)	0.544 (5)	0.504 (5)	0.205 (3)	11.2 (13)
H(6)	0.061 (4)	0.310 (4)	−0.213 (3)	6.7 (8)	H(101)	0.220 (4)	0.592 (4)	0.289 (3)	8.9 (10)
H(7)	0.188 (3)	0.457 (3)	−0.001 (2)	5.0 (7)	H(102)	0.363 (5)	0.634 (5)	0.354 (3)	11.6 (13)
H(8)	0.412 (5)	0.681 (5)	0.247 (3)	10.7 (12)	H(103)	0.418 (4)	0.782 (4)	0.392 (3)	9.7 (11)
H(111)	0.247 (4)	−0.334 (4)	−0.303 (3)	8.0 (10)	H(121)	0.186 (4)	−0.373 (4)	−0.478 (3)	9.5 (11)
H(112)	0.088 (4)	−0.332 (4)	−0.312 (3)	8.7 (10)	H(122)	0.193 (4)	−0.170 (4)	−0.375 (3)	9.2 (10)
H(0)	0.347 (3)	0.020 (3)	−0.130 (2)	3.2 (5)	H(123)	0.343 (4)	−0.155 (4)	−0.377 (3)	8.9 (10)

Table I (*Continued*)

c. $[Ni(ips)(NO_3)(DMF)]_2$

atom	x	y	z	B_{11}	B_{22}	B_{33}	B_{12}	B_{13}	B_{23}
Ni	0.07933 (6)	0.12473 (5)	−0.02197 (5)	3.19 (2)	1.84 (2)	2.02 (1)	0.34 (2)	1.63 (1)	0.22 (1)
O(1)	0.0462 (3)	0.0663 (3)	0.1345 (3)	3.91 (8)	2.0 (1)	2.36 (7)	0.22 (8)	2.20 (5)	−0.08 (8)
O(2)	0.0109 (4)	0.1987 (3)	−0.2350 (3)	4.81 (10)	3.5 (1)	3.26 (9)	0.82 (10)	2.67 (6)	0.69 (9)
O(4)	−0.2406 (6)	0.2784 (4)	−0.3888 (4)	7.27 (20)	6.4 (2)	3.92 (13)	2.34 (17)	2.09 (12)	3.07 (13)
O(3)	−0.1665 (4)	0.2042 (3)	−0.1717 (3)	4.19 (10)	3.3 (1)	3.52 (9)	0.76 (10)	2.38 (6)	0.74 (10)
O(5)	0.3117 (4)	0.0509 (3)	0.0630 (3)	4.28 (10)	3.1 (1)	2.83 (9)	1.10 (10)	1.94 (7)	0.44 (9)
N(1)	0.2117 (4)	0.3024 (3)	0.1158 (4)	3.0 (1)	2.2 (1)	2.9 (1)	0.3 (1)	1.74 (7)	0.6 (1)
N(2)	−0.1337 (5)	0.2284 (4)	−0.2684 (4)	4.9 (1)	2.6 (2)	2.5 (1)	0.4 (1)	1.72 (9)	0.7 (1)
N(3)	0.5191 (5)	−0.0642 (4)	0.2490 (4)	3.5 (1)	3.6 (2)	4.0 (1)	1.0 (1)	1.90 (9)	1.3 (1)
C(1)	0.1034 (5)	0.2863 (4)	0.2740 (4)	3.2 (1)	2.1 (2)	2.3 (1)	0.6 (1)	1.58 (8)	0.2 (1)
C(2)	0.0247 (5)	0.1503 (4)	0.2258 (4)	2.8 (1)	2.3 (2)	1.7 (1)	0.6 (1)	1.06 (8)	0.2 (1)
C(3)	−0.0660 (5)	0.1058 (5)	0.2825 (4)	3.9 (1)	2.7 (2)	2.6 (1)	0.1 (1)	2.11 (8)	−0.1 (1)
C(4)	−0.0791 (6)	0.1880 (5)	0.3838 (5)	4.5 (1)	4.0 (2)	3.4 (1)	0.6 (2)	2.81 (9)	0.4 (1)
C(5)	0.0015 (6)	0.3186 (5)	0.4364 (5)	6.4 (2)	3.3 (2)	4.1 (1)	1.2 (2)	3.94 (9)	−0.0 (1)
C(6)	0.0879 (6)	0.3653 (5)	0.3818 (5)	5.3 (2)	2.4 (2)	3.5 (1)	0.6 (1)	2.77 (10)	−0.2 (1)
C(7)	0.2000 (5)	0.3483 (4)	0.2258 (5)	3.8 (1)	2.0 (2)	2.5 (1)	0.3 (1)	1.64 (9)	−0.0 (1)
C(8)	0.3215 (6)	0.3843 (5)	0.0864 (5)	4.4 (1)	2.9 (2)	4.3 (1)	−0.2 (1)	3.00 (9)	0.0 (1)
C(9)	0.2230 (8)	0.4956 (6)	−0.0069 (6)	7.8 (2)	3.2 (2)	6.3 (2)	0.3 (2)	4.69 (13)	1.6 (2)
C(10)	0.5034 (8)	0.4334 (8)	0.2345 (8)	4.7 (2)	7.9 (4)	7.1 (2)	−0.8 (2)	3.34 (15)	1.5 (3)
C(11)	0.4098 (6)	0.0277 (5)	0.2023 (5)	3.9 (1)	3.5 (2)	3.1 (1)	0.5 (2)	2.01 (10)	0.3 (1)
C(12)	0.5182 (7)	−0.1526 (6)	0.1332 (7)	6.3 (2)	4.1 (2)	7.6 (2)	2.2 (2)	4.81 (13)	1.3 (2)
C(13)	0.6236 (10)	−0.0905 (8)	0.4120 (8)	6.6 (3)	9.2 (4)	5.0 (3)	3.5 (3)	2.12 (21)	3.3 (3)

atom	x	y	z	B, Å²	atom	x	y	z	B, Å²
H(3)	−0.112 (5)	0.019 (4)	0.258 (4)	2.4 (9)	H(101)	0.581 (6)	0.469 (6)	0.209 (6)	5.5 (13)
H(4)	−0.143 (5)	0.157 (4)	0.414 (4)	3.1 (10)	H(102)	0.560 (6)	0.367 (5)	0.285 (5)	5.4 (13)
H(5)	−0.005 (7)	0.374 (6)	0.489 (6)	6.8 (16)	H(103)	0.492 (6)	0.485 (5)	0.308 (5)	5.4 (13)
H(6)	0.135 (6)	0.452 (5)	0.419 (5)	4.9 (13)	H(121)	0.443 (6)	−0.126 (5)	0.035 (5)	5.9 (15)
H(7)	0.257 (5)	0.427 (4)	0.285 (4)	3.1 (10)	H(122)	0.624 (6)	−0.159 (6)	0.158 (5)	5.7 (14)
H(8)	0.328 (6)	0.326 (5)	0.020 (5)	4.7 (13)	H(123)	0.477 (6)	−0.235 (5)	0.140 (5)	5.7 (14)
H(11)	0.395 (6)	0.090 (5)	0.272 (5)	4.5 (12)	H(131)	0.604 (6)	−0.025 (6)	0.472 (6)	5.3 (13)
H(91)	0.286 (6)	0.549 (5)	−0.028 (5)	5.2 (13)	H(132)	0.570 (6)	−0.175 (5)	0.404 (5)	5.4 (13)
H(92)	0.083 (6)	0.463 (5)	−0.111 (5)	5.2 (13)	H(133)	0.750 (6)	−0.096 (5)	0.452 (5)	5.4 (13)
H(93)	0.203 (6)	0.558 (5)	0.045 (5)	5.4 (13)					

[a] The form of the anisotropic thermal parameter is $\exp[-(B_{11}a^{*2}h^2 + B_{22}b^{*2}k^2 + B_{33}c^{*2}l^2)/4 + (B_{12}a^*b^*hk + B_{13}a^*c^*hl + B_{23}b^*c^*kl)/2]$.

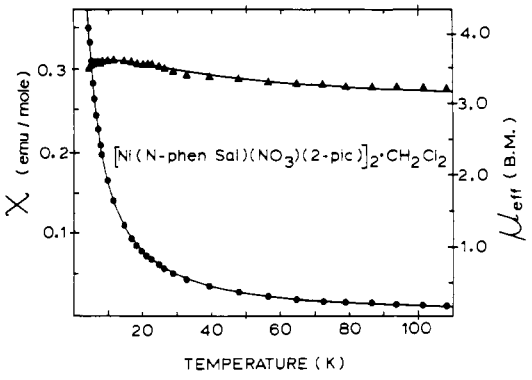

Figure 7. Plots of the magnetic susceptibility and effective magnetic moment of $[Ni(ps)(NO_3)(2\text{-pic})]_2 \cdot 2CH_2Cl_2$ as a function of temperature. The curves drawn represent the best fit of the magnetic data to $\chi(g,J,D,zJ')$ as described in the text. The complex has "cis" structure **2** and is an insulated ferromagnetic dimer (type a).

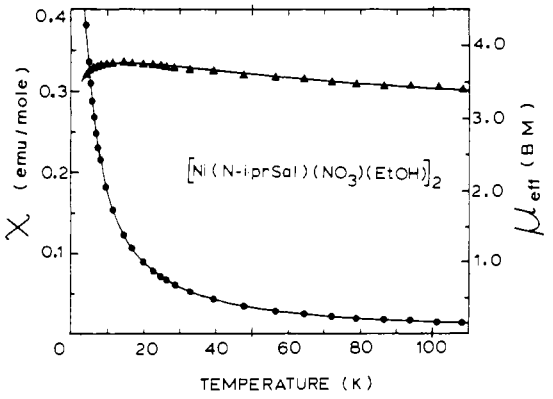

Figure 8. Plots of the magnetic susceptibility and effective magnetic moment of $[Ni(ips)(NO_3)(EtOH)]_2$ as a function of temperature. The complex has "cis" structure **2** and is a hydrogen-bonded ferromagnetic dimer (type b).

This Hamiltonian was applied to the Van Vleck equation[13] for the $S = 1$ basis wave function by Ginsberg et al.[14] The resulting magnetic susceptibility equation, $\chi(g,J,D,zJ')$, is a function of the zero-field splitting, D, and the intradimer electron spin-exchange term, J. An additional term, zJ', is included to represent the interdimer spin exchange. The equation is reproduced elsewhere[14] and therefore will not be included here. This equation was used for the analysis of the magnetic properties of all compounds.

The magnetic susceptibilities and effective magnetic moments of the three compounds are plotted as a function of temperature in Figures 7–9. In each case, the smooth line drawn through the points is the fit of the data to $\chi(g,J,D,zJ')$. The fitted parameters are listed in Table IV. Equally good fits of the data could be obtained with or without the interdimer exchange term (zJ'). The equation is insensitive to the D,zJ' combination; that is, within a large range, a change in the value of one parameter can be very readily compensated for by a change in the other parameter without damaging the quality of the fit. Since intermolecular hydrogen-bonded bridges are evident between the type b molecules, $[Ni_2(ips)_2(NO_3)_2(EtOH)_2]_\infty$, in the crystal lattice, both cases, with

(13) Van Vleck, J. H. "The Theory of Electric and Magnetic Susceptibilities"; Oxford University Press: London, 1932; p 182.
(14) Ginsberg, A. P.; Martin, R. L.; Brookes, R. W.; Sherwood, R. C. *Inorg. Chem.* **1972**, *11*, 2884.

Table II. Bond Distances (Å) for $[Ni(ps)(NO_3)(2\text{-pic})]_2$ (a), $[Ni_2(ips)_2(NO_3)_2(EtOH)_2]_\infty$ (b), and $[Ni(ips)(NO_3)(DMF)]_2$ (c)

	a	b	c		a	b	c
Ni-O(1)	2.002 (3)	1.983 (1)	1.990 (2)	C(8)-C(9)	1.381 (7)	1.423 (4)	1.515 (4)
Ni-O(1*)	2.060 (3)	2.053 (1)	2.065 (1)	C(8)-C(10)		1.309 (5)	1.550 (4)
Ni-O(2)	2.100 (3)	2.135 (1)	2.155 (2)	C(8)-C(13)	1.374 (7)		
Ni-O(3)	2.212 (3)	2.175 (2)	2.142 (2)	C(9)-C(10)	1.378 (7)		
Ni-O(5)		2.077 (2)	2.035 (2)	C(10)-C(11)	1.368 (8)		
Ni-N(1)	2.063 (4)	2.012 (2)	2.022 (2)	C(11)-C(12)	1.372 (7)	1.453 (5)	
Ni-N(5)	2.116 (4)			C(12)-C(13)	1.368 (8)		
O(1)-C(2)	1.338 (5)	1.341 (2)	1.345 (3)	C(14)-C(15)	1.381 (8)		
O(2)-N(2)	1.268 (5)	1.265 (2)	1.257 (3)	C(14)-C(19)	1.507 (9)		
O(3)-N(2)	1.263 (5)	1.254 (2)	1.273 (3)	C(15)-C(16)	1.352 (9)		
O(4)-N(2)	1.221 (5)	1.233 (2)	1.235 (3)	C(16)-C(17)	1.365 (9)		
O(5)-C(11)		1.423 (3)	1.241 (3)	C(17)-C(18)	1.388 (8)		
N(1)-C(7)	1.285 (6)	1.278 (3)	1.286 (3)	N(3)-C(11)			1.319 (3)
N(1)-C(8)	1.439 (5)	1.471 (3)	1.489 (3)	N(3)-C(12)			1.450 (4)
N(5)-C(14)	1.352 (6)			N(3)-C(13)			1.445 (4)
N(5)-C(18)	1.328 (6)			C-Cl(1)	1.75 (1)		
C(1)-C(2)	1.401 (6)	1.412 (3)	1.427 (3)	C-Cl(2)	1.66 (1)		
C(1)-C(6)	1.398 (6)	1.412 (3)	1.421 (3)	Ni-Ni*		3.010 (1)	3.083 (1)
C(1)-C(7)	1.453 (6)	1.446 (3)	1.433 (4)	O(4)-O(5)		2.768 (2)[a]	
C(2)-C(3)	1.399 (6)	1.382 (3)	1.390 (4)	O(4)-H(0)		2.14 (4)[a]	
C(3)-C(4)	1.375 (7)	1.378 (4)	1.369 (4)	O(4)-C(7)		3.453 (2)[b]	
C(4)-C(5)	1.371 (7)	1.364 (5)	1.381 (4)	C(2)-C(13)			3.397 (4)[c]
C(5)-C(6)	1.372 (7)	1.348 (4)	1.344 (4)				

[a] $1-x, -y, -z$. [b] $x, y-1, z$. [c] $1-x, -y, 1-z$.

Table III. Bond Angles (Deg) for $[Ni(ps)(NO_3)(2\text{-pic})]_2$ (a), $[Ni_2(ips)_2(NO_3)_2(EtOH)_2]_\infty$ (b), and $[Ni(ips)(NO_3)DMF]_2$ (c)

	a	b	c		a	b	c
O(1)-Ni-O(1*)	81.3 (1)	83.6 (1)	81.0 (1)	Ni-N(5)-C(14)	125.5 (3)		
O(1)-Ni-O(2)	166.5 (1)	160.6 (1)	157.9 (1)	Ni-N(5)-C(18)	115.9 (3)		
O(1)-Ni-O(3)	107.3 (1)	100.8 (1)	98.0 (7)	C(14)-N(5)-C(18)	118.2 (4)		
O(1)-Ni-O(5)		92.8 (1)	98.2 (1)	C(2)-C(1)-C(6)	120.1 (4)	117.8 (2)	117.0 (2)
O(1)-Ni-N(1)	87.8 (1)	91.9 (1)	91.8 (1)	C(2)-C(1)-C(7)	122.7 (4)	124.4 (2)	125.4 (2)
O(1)-Ni-N(5)	92.9 (1)			C(6)-C(1)-C(7)	117.0 (4)	117.8 (2)	117.6 (2)
O(1*)-Ni-O(2)	94.1 (1)		94.5 (1)	O(1)-C(2)-C(1)	122.7 (4)	122.1 (2)	120.4 (2)
O(1*)-Ni-O(3)	88.3 (1)		90.0 (1)	O(1)-C(2)-C(3)	119.6 (4)	119.1 (2)	121.3 (2)
O(1*)-Ni-O(5)			87.7 (1)	C(1)-C(2)-C(3)	117.7 (4)	118.8 (2)	118.3 (2)
O(1*)-Ni-N(1)	89.1 (1)		172.2 (1)	C(2)-C(3)-C(4)	121.0 (5)	120.7 (3)	121.8 (2)
O(1*)-Ni-N(5)	172.9 (1)			C(3)-C(4)-C(5)	121.2 (5)	121.2 (3)	120.8 (2)
O(2)-Ni-O(3)	59.6 (1)	59.9 (1)	60.2 (1)	C(4)-C(5)-C(6)	119.2 (5)	119.3 (3)	118.8 (2)
O(2)-Ni-O(5)		87.6 (1)	103.2 (1)	C(1)-C(6)-C(5)	120.8 (5)	122.2 (3)	123.3 (2)
O(2)-Ni-N(1)	104.9 (1)	107.4 (1)	93.3 (1)	N(1)-C(7)-C(1)	126.2 (4)	126.7 (2)	128.1 (2)
O(2)-Ni-N(5)	90.7 (1)			N(1)-C(8)-C(9)	119.8 (4)	114.2 (3)	110.2 (2)
O(3)-Ni-N(1)	164.1 (1)	167.0 (1)	94.0 (1)	N(1)-C(8)-C(10)		116.7 (3)	113.3 (2)
O(3)-Ni-N(5)	89.5 (1)			N(1)-C(8)-C(13)	121.4 (4)		
O(3)-Ni-O(5)		86.8 (1)	163.0 (1)	C(9)-C(8)-C(10)		128.7 (3)	113.2 (3)
O(5)-Ni-N(1)		90.2 (1)	90.4 (1)	C(9)-C(8)-C(13)	118.8 (4)		
Ni-O(1)-Ni*	98.7 (1)	96.4 (1)	99.0 (1)	C(8)-C(9)-C(10)	120.4 (5)		
Ni-O(1)-C(2)	118.9 (3)	119.4 (1)	123.7 (1)	C(9)-C(10)-C(11)	120.4 (5)		
Ni*-O(1)-C(2)	124.6 (3)	124.3 (1)	128.5 (1)	O(5)-C(11)-N(3)			123.6 (2)
Ni-O(2)-N(2)	94.7 (3)	92.2 (1)	91.4 (1)	C(10)-C(11)-C(12)	119.6 (5)		
Ni-O(3)-N(2)	89.7 (3)	90.6 (1)	91.6 (1)	C(11)-C(12)-C(13)	120.1 (5)		
Ni-O(5)-C(11)		125.9 (2)	120.7 (2)	C(8)-C(13)-C(12)	120.7 (5)		
Ni-N(1)-C(7)	120.3 (3)	120.4 (2)	121.6 (2)	N(5)-C(14)-C(15)	119.9 (5)		
Ni-N(1)-C(8)	123.4 (3)	122.8 (2)	119.4 (2)	N(5)-C(14)-C(19)	119.4 (5)		
C(7)-N(1)-C(8)	116.3 (4)	116.8 (2)	119.0 (2)	C(15)-C(14)-C(19)	120.6 (5)		
O(2)-N(2)-O(3)	116.0 (4)	117.3 (2)	116.8 (2)	C(14)-C(15)-C(16)	121.2 (6)		
O(2)-N(2)-O(4)	121.5 (5)	121.4 (2)	122.5 (3)	C(15)-C(16)-C(17)	119.5 (6)		
O(3)-N(2)-O(4)	122.6 (5)	121.3 (2)	120.7 (3)	C(16)-C(17)-C(18)	117.3 (6)		
C(11)-N(3)-C(12)			121.2 (2)	N(5)-C(18)-C(17)	123.8 (5)		
C(11)-N(3)-C(13)			120.6 (3)	O(5)-C(11)-C(12)		112.4 (3)	
C(12)-N(3)-C(13)			118.7 (3)	Cl(1)-C-Cl(2)	111.6 (5)		

and without zJ', are included for each of the three dimeric complexes. Since the magnetic equation is insensitive to the D,zJ' combination, the structural results are as important as the best fit of the magnetic data; the intermolecular hydrogen bonding observed in type b complexes is a strong indication that the intermolecular interaction represented by zJ' is not insignificant at least in this case. For the full range of possible fits, zJ' is always small, D is positive, though having a range of magnitudes, and J is essentially invariant. The equation is *very sensitive* to J, the intradimer exchange coupling constants, and therefore the J values *do give a realistic estimate* of the strength of the magnetic coupling.

By far the most striking result of the analysis of the magnetic data is the change in sign of the spin-exchange parameter J/K from +19 (case b, ferromagnetic) to −13 K (case c, antiferromagnetic), apparently due to the effect of the coordinating Lewis acid solvent molecule. Structurally this change in electron configuration is accompanied by a change in bonding configuration. Simply stated, in the DMF adduct (antiferromagnetic), the plane of the salicylaldimine ligand is coplanar with the Ni_2O_2 bridging plane, while in the ethanol adduct (ferromagnetic), the salicylaldimine plane is perpen-

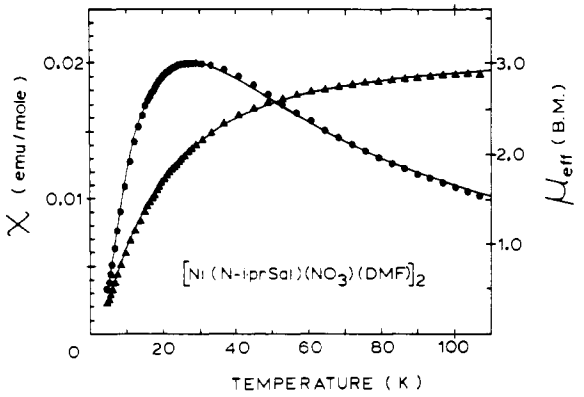

Figure 9. Plots of the magnetic susceptibility and effective magnetic moment of $[Ni(ips)(NO_3)DMF]_2$ as a function of temperature. The complex has "trans" structure **3** and is an antiferromagnetic dimer (type c).

Table IV. Parameters for the Fit of the Magnetic Data to the $\chi(g,J,D,zJ')$ Equation for $[Ni(R\text{-}sal)(NO_3)R']_2$

	R′ = 2-pic R = phenyl	R′ = EtOH R = isopropyl	R′ = DMF R = isopropyl
	i. $zJ' = 0$		
g	2.12 ± 0.02	2.19 ± 0.01	2.32 ± 0.01
J/k, K	13.0 ± 0.2	19.0 ± 0.5	−13.3 ± 0.1
(J, cm^{-1})	(9.0)	(13.2)	(−9.2)
D/k, K	7.9 ± 0.2	9.2 ± 0.5	17.0 ± 1.0
(D, cm^{-1})	(5.5)	(6.4)	(11.8)
	ii. $zJ' \neq 0$		
g	2.12 ± 0.02	2.15 ± 0.02	2.31 ± 0.02
J/k, K	12.5 ± 1.0	23.0 ± 1.0	−13.3 ± 0.05
(J, cm^{-1})	(8.7)	(16.0)	(−9.2)
D/k, K	19.2 ± 1.0	22.0 ± 1.0	16.0 ± 1.0
(D, cm^{-1})	(13.3)	(15.3)	(11.1)
zJ'/k, K	0.1 ± 0.1	0.3 ± 0.1	0.5 ± 0.1
(J', cm^{-1})	(0.07)	(0.14)	(0.3)

dicular to the Ni_2O bridging plane.

The major difference in the pathway of spin exchange is in the orientation of the electron orbitals on the bridging oxygens. In all three cases the Ni–O(1)–C(2) bonding angle is reasonably close to 120°. This angle indicates that oxygen is sp^2 hybridized with the p_z orbital probably involved in π overlap with the aromatic ring. In the antiferromagnetic case, all nickel–oxygen bridging σ bonds involve sp^2 hybrid orbitals on the oxygen and the $d_{x^2-y^2}$ orbital on the nickel. In addition there may also be a significant π overlap between the nickel d_{z^2} orbitals and the oxygen p_z orbital. In the ferromagnetic case, one nickel–oxygen σ bond uses an sp^2 oxygen orbital and the other nickel–oxygen σ bond uses a p_z oxygen orbital. There is no π overlap possible between the two nickel(II) centers for this case.

The electron orbital overlap integral for the magnetic exchange may be expressed as a combination of σ and π contributions having the form $\langle (Ni)3d_{x^2-y^2}\|(O)sp^2\|(Ni')3d_{x^2-y^2}\rangle$ and $\langle (Ni)3d_{xz}\|(O)p_z\|(Ni')3d_{z^2}\rangle$ for the antiferromagnetic case, and the σ-bonding pathway $\langle (Ni)3d_{x^2-y^2}\|(O)sp^2\perp(O)p_z|(Ni)3d_{z^2}\rangle$ for the ferromagnetic case. The notation for these electron orbital overlap expressions is defined elsewhere.[15,16] The symbols | and $\perp$ represent magnetically compatible and magnetically orthogonal overlap, respectively.

The magnetic orthogonality principle of the orbital symmetry relationships has been used to predict the sign and magnitude of the magnetic exchange.[15,16] The presence of magnetic orthogonality in the overlap integral ($\perp$) is one of the conditions that will permit ferromagnetic exchange. The observed exchange pathways obtained from the crystal structures and the complementary magnetic data are easily correlated with the symmetry relationships of the bridging orbitals on the phenolic oxygen.

In the case where one Ni–O bridging bond involves a p_z oxygen orbital (cis, cases a and b), the expected ferromagnetic interaction is observed. On the other hand, the effectiveness of the σ, π overlap integral in propagating antiferromagnetic exchange is evident from the observed strong antiferromagnetic coupling of the two nickel(II) centers.

Acknowledgment. Support under NSF Grant CHE77-01372, and from the Research Corp., is gratefully acknowledged.

Registry No. $[Ni(ps)(NO_3)(2\text{-pic})]_2\cdot 2CH_2Cl_2$, 78199-16-3; $Ni_2(ips)_2(NO_3)_2(EtOH)_2$, 78199-17-4; $[Ni(ips)(NO_3)DMF]_2$, 78199-18-5; $Ni(ps)_2$, 38929-70-3; $Ni(ips)_2$, 41754-10-3.

Supplementary Material Available: Tables of magnetic susceptibilities, analytical data, and observed and calculated structure factors (30 pages). Ordering information is given on any current masthead page.

(15) Ginsberg, A. P. *Inorg. Chim. Acta, Rev.* **1971**, *5*, 45.
(16) Anderson, P. W. *Magnetism* **1963**, *1*.

Contribution from the Department of Chemistry, University of Maine, Orono, Maine 04469

Laser-Excited Luminescence and Absorption Study of Monomer and Cluster Tetracyanopalladate(II) Species in Mixed Crystals

A. KASI VISWANATH, JEANETTE VETUSKEY, WILLIAM D. ELLENSON, MARY BETH KROGH-JESPERSEN, and HOWARD H. PATTERSON*

Received January 13, 1981

Laser-excited luminescence studies of $Pd(CN)_4^{2-}$ ions doped in NaCl crystals have demonstrated the existence of $Pd(CN)_4^{2-}$ clusters with the luminescence similar to that from single crystals of $BaPd(CN)_4\cdot 4H_2O$. Also, for mixed crystals of NaCN and KCN, luminescence from $Pd(CN)_4^{2-}$ clusters was observed. The optical absorption and MCD spectra of monomer species in palladium-doped crystals of alkali halides were assigned on the basis of MO calculations. The separation of the a_{2u} and e_u electronic states for $Pd(CN)_4^{2-}$ in alkali halides was found to be greater than that for $Pd(CN)_4^{2-}$ in solution.

Introduction

The tetracyanide compounds of Ni, Pd, and Pt in the solid state form polymer chains with metal–metal bonding and show unusual properties which are not found in their aqueous solutions.[1-10] The best example among the tetracyanides is $K_2Pt(CN)_4Br_{0.3}\cdot 3H_2O$ (KCP) which has a large electrical conductivity at room temperature.[3] There are no palladium

(1) J. S. Miller and A. J. Epstein, *Prog. Inorg. Chem.*, 20 (1976).
(2) K. Krogmann, *Angew. Chem., Int. Ed Engl.*, **8**, 38 (1969).

0020-1669/81/1320-3493$01.25/0